Severe Mycobacterial Immune Reconstitution Inflammatory Syndrome (IRIS) in Advanced Human Immunodeficiency Virus (HIV) Has Features of Hemophagocytic Lymphohistiocytosis and Requires Prolonged Immune Suppression

Joseph M. Rocco,[1] Elizabeth Laidlaw,[1] Frances Galindo,[1] Megan Anderson,[1] Adam Rupert,[2] Jeanette Higgins,[2] Ornella Sortino,[1] Ana M. Ortega-Villa,[1] Virginia Sheikh,[1] Gregg Roby,[1] Safia Kuriakose,[1] Andrea Lisco,[1] Maura Manion,[1] and Irini Sereti[1]

[1]National Institute of Allergy and Infectious Diseases, National Institutes of Health, Bethesda, Maryland, USA; and [2]Leidos Biomedical Research, Inc, Frederick, Maryland, USA

Background. People with HIV and mycobacterial infections can develop immune reconstitution inflammatory syndrome (IRIS) after starting antiretroviral therapy (ART). Severe mycobacterial IRIS has an overlapping clinical phenotype with hemophagocytic lymphohistiocytosis (HLH). We evaluated the pathophysiologic similarities between mycobacterial IRIS and HLH to identify clinical and immune predictors of mycobacterial IRIS severity.

Methods. HLH criteria were applied to a longitudinal cohort of 80 patients with HIV (CD4 <100 cells/μL) and mycobacterial infections. Participants were subdivided into IRIS meeting HLH criteria (HLH-IRIS), IRIS without HLH (IRIS), and those without IRIS (non-IRIS). Clinical outcomes were evaluated by regression analyses. Soluble biomarkers and T-cell subsets were assessed at baseline and IRIS-equivalent time points.

Results. HLH-IRIS patients required corticosteroids more frequently (OR: 21.5; 95%CI: 5.6–114.8) and for longer duration (21.2; 95%CI: 10.7–31.7 weeks) than those not meeting HLH criteria. Utilizing decision tree analyses, hemoglobin <9.2 g/dL was the best predictor of HLH-IRIS before ART, whereas ferritin, CXCL9 and sCD25 were most diagnostic for HLH at IRIS onset. At the IRIS timepoint, but not baseline, HLH-IRIS patients had lower regulatory and higher activated T cells along with greater production of IFNγ–IL-18 axis biomarkers compared with both IRIS and non-IRIS groups. Principal component analysis corroborated the distinct clustering of HLH-IRIS patients.

Conclusions. Severe mycobacterial IRIS and HLH have an overlapping pathogenesis involving IFNγ and unopposed T-cell activation causing severe inflammatory disease clinically distinguished by hyperferritinemia (hyperferritinemic IRIS [FIRIS]). Hemoglobin, ferritin, CXCL9, and sCD25 identify high-risk patients and may improve risk stratification and therapeutic strategies for mycobacterial IRIS.

Keywords. human immunodeficiency virus; tuberculosis; mycobacteria; immune reconstitution inflammatory syndrome; macrophage activation syndrome.

In people with human immunodeficiency virus (PWH), immune reconstitution inflammatory syndrome (IRIS) represents a paradoxical worsening of manifestations or unmasking of an underlying infection or malignancy after starting antiretroviral therapy (ART). Mycobacterial diseases (tuberculosis [TB] or nontuberculous mycobacteria [NTM]) represent the most common opportunistic infection predisposing to IRIS [1]. Interestingly, inflammatory paradoxical reactions were originally described after antibiotic initiation in individuals with *Mycobacterium tuberculosis* in the absence of human immunodeficiency virus (HIV) [2]. Late presentations of HIV with low CD4 counts and mycobacterial infections are common, particularly in resource-constrained settings, and IRIS severity can range from mild exacerbation of infection to severe disease requiring hospitalization and protracted courses of corticosteroids.

Current treatment guidelines recommend ART initiation within 2 weeks of starting anti-TB treatment in people with TB and low CD4 counts, leading to higher rates of paradoxical TB-IRIS [3, 4]. Optimal management of these patients requires a delicate balance of preserving immune recovery while limiting immune-mediated pathology. Identifying prognostic markers of mycobacterial IRIS is an unmet clinical need and could aid in the management of this complex syndrome.

The pathogenesis of mycobacterial IRIS includes increased monocyte/macrophage activation through inflammasome pathways leading to greater interleukin (IL)-1ß/IL-18 production [5–8], in combination with an expansion of polyfunctional, mycobacteria-specific, cytotoxic CD4 T cells [9, 10]. High pathogen burden is known to increase risk [11]. Biomarker profiles in mycobacterial IRIS are characterized by increased IL-6, IL-10, IL-27, soluble CD14 (sCD14), and interferon-γ (IFNγ) [12–14]. TB-IRIS specifically is associated with increased production of IL-18, IL-18 binding protein (IL-18BP), and sCD163 [6].

Clinically, mycobacterial IRIS has overlapping features with hemophagocytic lymphohistiocytosis (HLH), another hyperinflammatory syndrome characterized by fevers, cytopenias, and hyperferritinemia. Primary HLH (pHLH) is caused by genetic defects along the cytotoxicity pathway, leading to immune dysregulation, hypercytokinemia, and multiorgan failure [15]. Secondary HLH (sHLH) occurs later in life as a robust inflammatory response triggered by autoimmune diseases (referred to as macrophage activation syndrome (MAS) infections or malignancies [16, 17]. The pathophysiology of HLH is primarily driven by dysregulated, hyperactive T cells with a pathologic production of IFNγ [15]. This unique IFNγ signature and activated T-cell phenotype is specific for HLH and differentiates it from sepsis and other hyperinflammatory syndromes [18–20]. A similar biomarker profile has been identified in sHLH triggered by malignancies or autoimmunity [21, 22].

Recognizing the similarities between mycobacterial IRIS and sHLH, we retrospectively applied HLH/MAS criteria to a longitudinal cohort of PWH and mycobacterial infections. Detailed immune profiling including biomarkers and T-cell phenotyping was performed to evaluate for overlapping pathophysiology between these hyperinflammatory syndromes and to identify clinically relevant markers that could be used to improve risk stratification and highlight potential therapeutic targets.

METHODS

Eighty PWH with mycobacterial infections were previously enrolled in 1 of 2 institutional review board approved observational, prospective studies (NCT00286767, NCT02147405) of IRIS in people with HIV and CD4 count less than 100 cells/µL (Supplementary Methods). All patients were evaluated at the National Institutes of Health (NIH). Patients could also enroll if they were on ART presenting with symptoms consistent with IRIS, regardless of CD4 count. Participants had samples collected before ART initiation, except in those enrolling during an IRIS event (n = 14), and longitudinally thereafter at weeks 2, 4, 8, and 12. All participants signed an informed consent and procedures were in accordance with the Declaration of Helsinki.

Clinical Description
Mycobacterial infections were diagnosed based on clinical and histologic and/or microbiologic evidence. IRIS events were defined using the AIDS Clinical Trials Group (ACTG) IRIS definition criteria [1]. ART and antibiotic drug levels were performed when needed to confirm medication adherence and absorption for IRIS ascertainment and to exclude inadequately treated mycobacterial infection. Patients meeting clinical-laboratory criteria for HLH/MAS at or immediately before IRIS onset formed the HLH-IRIS group. The IRIS group included patients who developed IRIS without meeting HLH/MAS criteria and the non-IRIS group those who did not develop IRIS. We utilized all published HLH/MAS criteria [23–25] (Supplementary Table 1), including the American College of Rheumatology MAS criteria, to broadly capture an HLH/MAS clinical phenotype. Macrophage activation syndrome pathogenesis shares similarities with mycobacterial IRIS including involvement of innate immune signaling, increased IL-18 production, and inflammasome activation [5, 6, 16]. Notably, few patients had bone marrow biopsies; however, hemophagocytosis is neither sensitive nor specific for the diagnosis of HLH/MAS, and thus unlikely to affect our classification [26, 27].

Immune Profiles
Plasma samples were available for 73 patients at IRIS onset (IRIS time point) and for 58 patients pre-ART (baseline time point). We selected the IRIS time point as the time when clinical IRIS criteria were met: week 2 (n = 17), week 4 (n = 19), and week 8 (n = 16), with 2 patients developing IRIS over 8 weeks after starting ART. Since the median onset of IRIS occurred at week 4, this time point was used as the "IRIS-equivalent time point" for the non-IRIS group. Soluble biomarkers were chosen based on their association with IRIS or HLH/MAS [15, 16]: C-reactive protein (CRP), IL-1ß, IL-6, soluble tumor necrosis factor α receptor I (sTNFα-RI), granulocyte-macrophage colony–stimulating factor (GM-CSF), sCD25, C-X-C motif chemokine ligand (CXCL) 9 (CXCL9), CXCL10, IFNγ, IL-10, IL-12, IL-18, IL-18BP, sCD163, C1q, C3a, C5a, CH50, and S100A12 at baseline and IRIS time points (Supplementary Methods).

T-cell immunophenotyping was performed by a standardized procedure at each time point. Flow panels included T-cell markers (CD3, CD4, CD8) and activation markers (CD38, HLA-DR). Markers for regulatory T cells (Tregs; CD25, FOXP3) were also included in protocol NCT00286767. For those enrolled in NCT02147405, additional flow cytometry for Tregs was performed using available stored samples (Supplementary Methods).

Statistical Analyses
Analyses of biomarkers from baseline and IRIS-equivalent time points were performed using medians and interquartile range (IQR) and comparisons across groups were made with Kruskal–Wallis test. Statistically significant ($P < .05$) differences were further evaluated with pairwise Wilcoxon and Holm

correction. Spearman correlation matrices were generated using biomarker results from the IRIS time point. Decision trees and principal component analyses were performed in R (version 4.1.2; R Foundation for Statistical Computing) with details provided in the Supplementary Methods. Regression analyses were used to determine the impact of HLH-IRIS on disease outcomes.

RESULTS

Clinical Characteristics

Overall, 80 PWH with mycobacterial infections were followed longitudinally from 2006 to 2021. The median age at enrollment was 38 years (range: 25–58 years), with more men (n = 52) than women (n = 28) (Table 1). The majority of participants were Black (African or African-American) (n = 50) or White/Hispanic (n = 20). All participants had a baseline CD4 count of less than 100 cells/μL (median: 32; IQR: 11–66). Mycobacterial infections were primarily due to *M. tuberculosis* (n = 36) or *Mycobacterium avium* complex (MAC; n = 34).

In total, 54 (67.5%) patients developed mycobacterial IRIS meeting ACTG criteria; therefore, 26 (32.5%) individuals were included into the non-IRIS group. IRIS episodes were paradoxical in 24 (44%) and unmasking in 30 (56%). Of these 54 patients with IRIS, 26 (32.5%) met published criteria for HLH/MAS [23–25] and were classified into the HLH-IRIS subgroup, leaving 28 (35%) patients in the IRIS group (without HLH/MAS). There was no significant difference in age, sex, presence of disseminated mycobacterial infection, CD4 T cells, or body mass index at baseline between the 3 groups. Four patients with HLH-IRIS were coinfected with disseminated histoplasmosis and 2 others had concomitant Kaposi sarcoma (KS)–associated herpesvirus inflammatory syndromes. There was no difference in rates of KS between the groups.

Clinical laboratory tests at IRIS onset are shown in Supplementary Table 2. In the HLH-IRIS group, 11 (42.3%) met more than 1 HLH/MAS criteria, with 16 (61.5%) meeting MAS criteria and 14 (53.9%) meeting the H-score cutoff of 169 for sHLH, whereas 13 (50%) fulfilled the HLH 2004 criteria. Ferritin and hemoglobin were markedly abnormal in the HLH-IRIS group with a median ferritin of 1383 ng/mL (IQR: 1002–1756 ng/mL) and hemoglobin 8.4 g/dL (IQR: 7.5–9.1 g/dL). There were no differences in HIV plasma levels or detectable cytomegalovirus. Circulating Epstein-Barr virus was common, but there was no difference in the levels of viremia between groups (Supplementary Table 2).

Patients With HLH-IRIS Demonstrate a Prominent IFNγ Inflammatory Profile During IRIS

Biomarker profiles were examined at baseline (n = 58) and IRIS time points (n = 73). All values were standardized with medians and IQRs. Pre-ART, fold-differences between the groups

demonstrated higher sCD25, IL-6, and ferritin levels in groups with HLH-IRIS compared with those with IRIS without HLH (Figure 1*A*). To determine which biomarkers could predict patients who would develop HLH-IRIS, a decision-tree analysis was performed that identified hemoglobin of less than 9.2 g/dL as the best baseline predictor of HLH-IRIS (Figure 1*B*).

At IRIS onset, there was a strong increase in IFNγ and its downstream markers (CXCL9, CXCL10, IL-18BP) in patients with HLH-IRIS compared with those with IRIS without HLH (Figure 2*A*). The T-cell activation marker, sCD25, and IL-18, a cytokine that stimulates IFNγ production, were also significantly elevated in HLH-IRIS compared with the IRIS subgroup. Increased levels of a broad range of inflammatory markers were noted in the HLH-IRIS cohort compared with the non-IRIS cohort. No IFNγ signature was observed when the IRIS cohort was compared with the non-IRIS cohort. Change in biomarker levels from baseline to IRIS onset identified a significant increase in CRP, IL-6, and IL-1ß in both the IRIS and HLH-IRIS groups (Supplementary Figure 1). However, only the HLH-IRIS cohort demonstrated a statistically significant increase in IFNγ, CXCL9, and IL-18BP at the IRIS time point (Supplementary Figure 2). Correlation network analyses identified a balanced network in the non-IRIS group with multiple correlations between myeloid and T-cell activation markers (Figure 2*B*), which were absent in the IRIS group. The HLH-IRIS group, however, showed a redistribution of inflammatory pathways with amplification of associations between CXCL10 with sCD163 and sCD25. Ferritin correlated with IL-18, and both correlated inversely with hemoglobin.

Decision-tree analysis was repeated using biomarkers from the IRIS time point. This identified CXCL9 greater than 1280.8 pg/mL as the strongest marker of HLH-IRIS, with a second branch at sCD25 greater than 3375.6 pg/mL, which could accurately classify most patients with HLH-IRIS (Figure 3*A*). To identify which biomarkers could best predict need for long-term immune suppression (>8 weeks), another decision tree was modeled and identified sCD25 greater than 3953.6 pg/mL as the best predictor for this outcome (Figure 3*B*). A final decision tree was performed using all available clinical laboratory tests, which identified ferritin greater than 841 ng/mL during IRIS as the best predictor of HLH-IRIS, with baseline hemoglobin of less than 9.2 g/dL as the second-best classifier (Figure 1*C*).

Activated T Cells Are Expanded in HLH-IRIS With Decreased Regulatory T Cells

We found no difference in CD4 and CD8 T cells between the groups at baseline (Supplementary Figure 3*A*, 3*B*, 3*D–E*) or at the IRIS time point (Figure 4*A*, 4*B*, 4*D–E*). There was a statistically significant increase in both CD4$^+$D38$^+$DR$^+$ and CD8$^+$CD38$^+$DR$^+$ T cells in the patients with HLH-IRIS compared with IRIS and non-IRIS groups during the IRIS time

Table 1. Clinical Characteristics at Enrollment Across the 3 Groups

Characteristics	HLH-IRIS (n = 26)	IRIS (n = 28)	No IRIS (n = 26)	P
Age, y	37 (33.3–41.8)	38.5 (29.8–45.3)	40 (37.3–44.8)	.27
Female, n (%)	12 (46.2)	6 (21.4)	10 (38.5)	.15
BMI, kg/m^2	21.8 (18.9–24.8)	22.1 (20.2–24.1)	23.1 (21–26.4)	.24
Race/ethnicity, n (%)				
White/Hispanic	5 (19.2)	9 (32.1)	6 (23.1)	.53
Black	21 (80.8)	12 (42.9)	17 (65.4)	.015
Other[a]	0 (0)	7 (25)	3 (11.5)	.021
Mycobacteria, n (%)				
Mycobacterium tuberculosis	14 (53.8)	8 (28.6)	15 (57.7)	.064
Mycobacterium avium	10 (38.5)	17 (60.7)	6 (23.1)	.018
Other[b]	2 (7.7)	3 (10.7)	4 (15.4)	.76
Disseminated mycobacterial infection , n (%)	19 (73.1)	16 (57.1)	13 (50)	.22
Histoplasmosis, n (%)	4 (15.4)	0 (0)	0 (0)	…
Malignancy, n (%)				
Lymphoma	0 (0)	3 (10.7)	0 (0)	…
Kaposi sarcoma	2 (7.7)	2 (7.1)	1 (3.8)	…
KSHV (MCD, KICS)	2 (7.7)	0 (0)	0 (0)	…
CD4 T cells/μL prior to antiretroviral treatment	44 (9–66)	30 (13–45)	35 (17–79)	.45
CD4 T cells/μL[c]	91 (62–171)	114 (49.5–160)	101 (44.5–156)	.88
CD8 T cells/μL[c]	387 (274–744)	598 (335–802)	623 (427–1014)	.51
CD4-to-CD8 T-cell ratio[c]	0.18 (0.05–0.36)	0.20 (0.12–0.32)	0.17 (0.09–0.35)	.66
C-reactive protein,[c] mg/L	87.6 (33.5–135)	47.3 (24.7–89.9)	8.0 (4.0–15.3)	<.001
Ferritin,[c,d] ng/mL	1383 (1002–1756)	265 (135–582)	242 (86.5–625)	<.001

Data represent medians with interquartile ranges (age) and frequencies (female sex, race, mycobacteria, disseminated infection). The Kruskal–Wallis test was used to compare continuous variables between the groups, while the Pearson's χ² test was used to compare frequencies.

Abbreviations: BMI, body mass index; HLH, hemophagocytic lymphohistiocytosis; IRIS, immune reconstitution inflammatory syndrome; KICS, Kaposi's sarcoma herpesvirus inflammatory cytokine syndrome; KSHV, Kaposi's sarcoma herpesvirus; MCD, multicentric Castleman's disease.

[a]Other races include White/Caucasian (n = 8) and Asian (n = 2).

[b]Other mycobacterial infections were due to *Mycobacterium kansasii* (n = 6), *Mycobacterium genavense* (n = 2), *Mycobacterium marinum* (n = 1), and *Mycobacterium bovis* (n = 1).

[c]Laboratory values from the IRIS time point or equivalent week 4 time point.

[d]Healthy control range for ferritin: men—12–300 ng/mL; women—12–150 ng/mL.

point but not pre-ART (Figure 4C and 4F; Supplementary Figure 3C and 3F). A depletion of Tregs has also been implicated in HLH pathogenesis [28], and we found a decrease in Tregs (CD4$^+$CD25$^+$FOXP3$^+$) in the HLH-IRIS group (Figure 4G).

The ratio of activated CD4 T cells to Tregs demonstrated an imbalance in these subsets in the HLH-IRIS group compared with the others (Figure 4H and 4I). This dysregulated immunophenotype was not present at baseline, suggesting that it occurred during T-cell reconstitution after ART initiation (Supplementary Figure 3G–I). Since shedding of CD25 can occur in hyperinflammatory states, we also looked at CD4$^+$FOXP3$^+$ T cells, which gave consistent results (Supplementary Figure 4). Finally, there was no significant decrease in the degree of CD25 expression as measured by fluorescence intensity in the HLH-IRIS group.

To further validate the distinct immune profile of the HLH-IRIS subgroup, a principal component analysis (PCA) was performed incorporating the IFNγ–IL-18 axis biomarkers and T-cell immunophenotypes at the IRIS time point (Figure 5). This revealed a marked overlap between the non-IRIS and IRIS groups. The HLH-IRIS population, however, formed a distinct cluster, emphasizing the unique immune dysregulation driven by T-cell activation and pathologic IFNγ production in this group.

Immune Profile of Patients With Tuberculosis Versus Nontuberculous Mycobacterial Infections

Immune profiles of those with TB versus NTM infections at baseline or the IRIS-equivalent time points did not differ significantly, although small biomarker differences were noted (Supplementary Figures 5 and 6). In patients with mycobacterial IRIS, those with TB had increased complement, monocyte activation, and IFNγ-associated markers; however, in the HLH-IRIS group, there was no difference in biomarker or T-cell profiles by PCA. In addition, immune profiles in disseminated compared with localized mycobacterial infection again overlapped; however, there was a trend towards higher inflammatory markers in disseminated infection (Supplementary Figure 7A and 7B).

Patients With HLH-IRIS Have Severe and Protracted Inflammatory Disease

Logistic and linear regression was performed to evaluate the need for corticosteroid treatment and duration of immune suppression. Corticosteroids were used as first-line treatment for
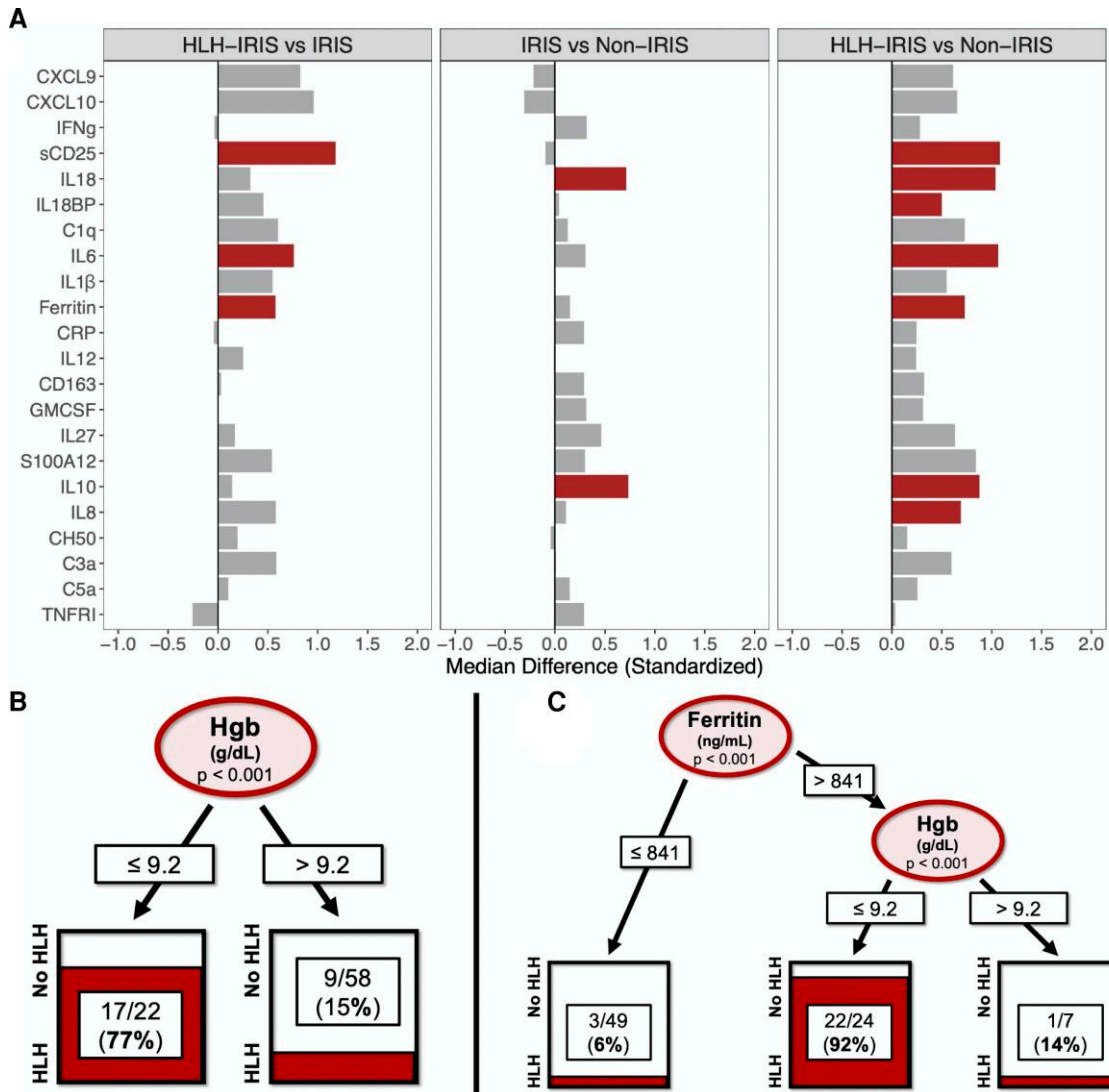
Figure 1. Comparison of biomarkers at the baseline time point between the groups and decision-tree analyses for HLH-IRIS using biomarkers or clinical variables. *A*, Biomarkers were standardized using median and interquartile ranges, and bar plots are displayed as fold-differences between groups. Differences that reached statistical significance after adjustment for multiple comparisons (adjusted *P* < .05) are represented in colored bars. There was no increase in IFNγ or its associated markers in the HLH-IRIS group. Soluble CD25, IL-6, and ferritin remained elevated when HLH-IRIS was compared with both the IRIS and non-IRIS groups. Only IL-10 and IL-18 were elevated in both the HLH-IRIS and IRIS groups when compared with the non-IRIS group. Decision trees predicting HLH-IRIS were performed using (*B*) all available clinical laboratory tests, which included baseline hemoglobin and clinical laboratory values at IRIS onset (white blood cell count, hemoglobin, platelets, ferritin, fibrinogen, triglycerides, and aspartate aminotransferase), and (*C*) all 14 markers used in the initial decision tree (IFNγ, CXCL9, CXCL10, IL-18, IL-18BP, sCD25, CD163, IL-6, CRP, IL-10, IL-27, C1q, hemoglobin, ferritin), except from the baseline time point. Potential splits are only included in the tree model if they met the Bonferroni-adjusted *P* value for statistical significance (*P* < .05). Ovals indicate a split in the prediction rule on a specific variable, along with the corresponding *P* value. Each square shows the percentage of observations within that branch that met the outcome variable. Hemoglobin values are represented as g/dL and ferritin as ng/mL. Abbreviations: BP, binding protein; CRP, C-reactive protein; CXCL, C-X-C motif chemokine ligand; GMCSF, granulocyte-macrophage colony–stimulating factor; Hgb, hemoglobin; HLH, hemophagocytic lymphohistiocytosis; IFNγ (IFNg), interferon-γ; IL, interleukin; IRIS, immune reconstitution inflammatory syndrome; sCD25, soluble CD25; TNFRI, tumor necrosis factor α receptor I.

all patients. Those meeting HLH/MAS criteria were significantly more likely to require corticosteroids with an odds ratio (OR) of 21.5 (95% confidence interval [CI]: 5.6–114.8) after controlling for age, sex, race, mycobacterial species, CD4 T cells, and disseminated infection. Duration of immune suppression was initially evaluated using the binary outcome of steroid treatment for greater than 8 weeks, as this is often the

time when steroid-sparing agents are considered when managing chronic inflammatory conditions. When controlling for the same covariates, patients with HLH-IRIS had an OR of 27.7 (95% CI: 6.5–165.7) for requiring corticosteroids for more than 8 weeks. The total duration of immune suppression was quantified using linear regression (controlling for the same covariates), with patients with HLH-IRIS requiring immune
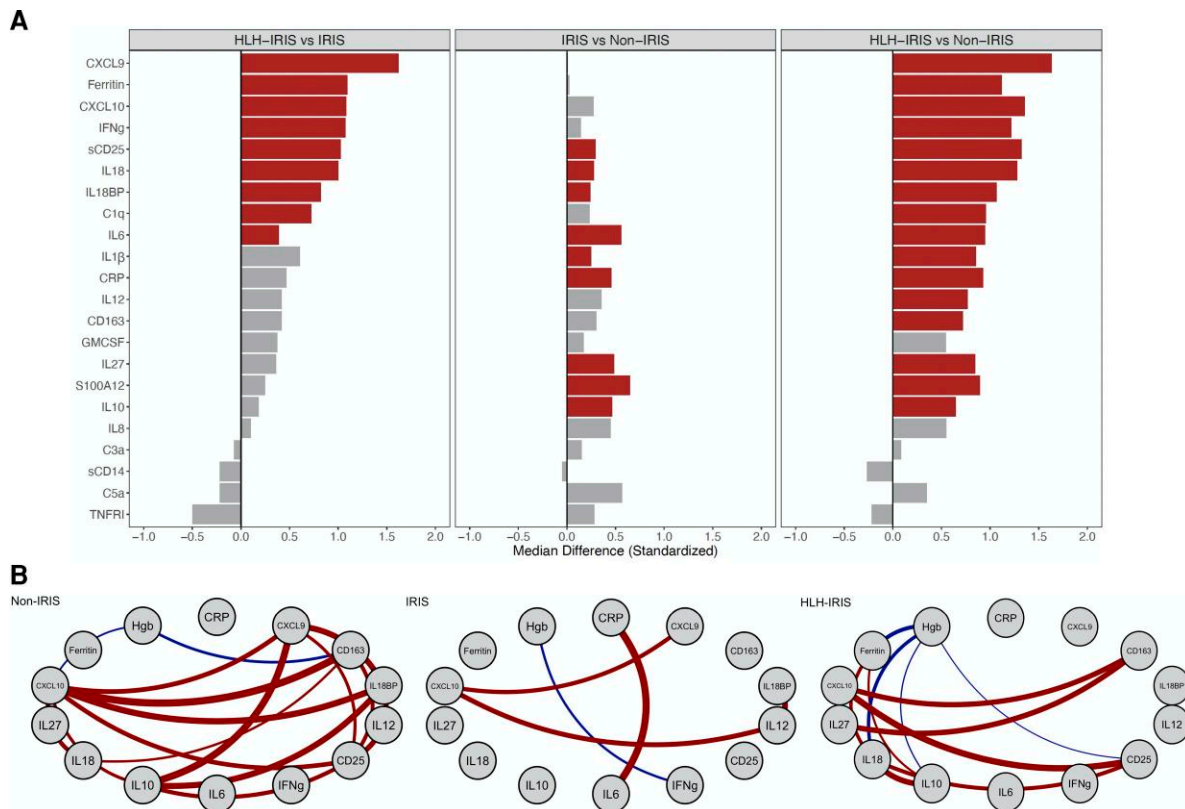
Figure 2. Comparison of biomarkers between the groups at the IRIS time point and Spearman correlation network analyses of each group at IRIS onset or the week 4 time point. *A,* Biomarkers were standardized using medians and interquartile ranges, and bar plots are displayed as fold-differences between groups. Differences that reached statistical significance after adjustment for multiple comparisons (adjusted $P < .05$) are represented as colored bars. A strong IFNγ signature (IFNγ, CXCL9, CXCL10, IL-18BP) was noted in the HLH-IRIS group when compared with the IRIS and non-IRIS groups. Comparison between IRIS and non-IRIS groups showed an absence of this IFNγ signature but differences in innate immune/myeloid activation markers (CRP, IL-6, IL-10, IL-27). *B,* Spearman correlation network analyses were performed within each group. Connecting lines represent statistically significant correlations ($P < .001$) with a correlation coefficient of $r > 0.4$ or $r < -0.4$. Red connecting lines represent positive correlations while blue lines infer negative correlations. Significant differences in inflammatory networks were identified with a balanced pattern of correlations in the non-IRIS group, which dramatically decreased in the patients with IRIS. Only the IRIS group demonstrated a strong correlation between CRP and IL-6. The HLH-IRIS group showed a redistribution of the inflammatory network with significant associations between CXCL10 with CD163 and sCD25. Ferritin correlated strongly with IL-18 and both of these markers were negatively associated with hemoglobin. Abbreviations: BP, binding protein; CRP, C-reactive protein; CXCL, C-X-C motif chemokine ligand; GMCSF, granulocyte-macrophage colony–stimulating factor; Hgb, hemoglobin; HLH, hemophagocytic lymphohistiocytosis; IFNγ (IFNg), interferon-γ; IL, interleukin; IRIS, immune reconstitution inflammatory syndrome; sCD25, soluble CD25; TNFRI, tumor necrosis factor α receptor I.

suppression for 21.2 weeks (95% CI: 10.7–31.7 weeks) more than those not meeting HLH/MAS criteria. In fact, 8 of the 26 patients (30.8%) with HLH-IRIS required additional immunosuppressive agents (infliximab, tocilizumab) to control refractory inflammation and limit steroid-associated adverse effects (Supplementary Table 3). No patients in the IRIS group required immunosuppression beyond corticosteroids.

DISCUSSION

Defining the pathophysiology of mycobacterial IRIS and identifying predictive markers of disease severity remain essential, especially for areas with high rates of HIV and TB coinfection. In our well-characterized, longitudinal cohort of PWH with mycobacterial infections, we identified that one-third developed severe IRIS meeting HLH/MAS criteria. This HLH-IRIS subgroup had a distinct clinical course requiring more corticosteroids and a longer duration of immunosuppression, with one-third of them requiring additional treatment beyond corticosteroids due to refractory inflammation or intolerance.

Immune profiles prior to ART were similar between groups, as uncontrolled HIV viremia and other opportunistic infections overwhelmingly drive inflammation. The HLH-IRIS and IRIS cohorts did demonstrate higher monocyte activation (IL-18, IL-6, ferritin), potentially primed by the unrestrained mycobacterial infection; however, systemic increases in IFNγ and its associated markers occurred only during ART-mediated T-cell reconstitution in the HLH-IRIS cohort at the onset of the clinical HLH phenotype (proposed model in Supplementary Figure 8). This unique IFNγ signature at HLH onset resembled the pattern reported in primary and secondary HLH, supporting the key role of IFNγ in its
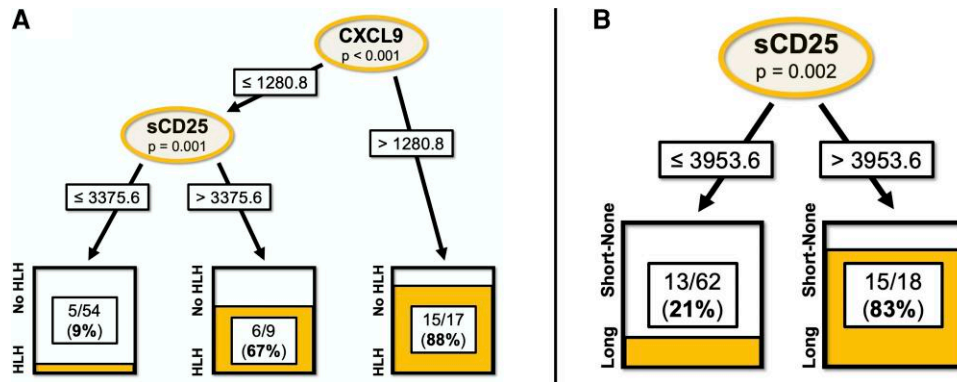
Figure 3. Decision-tree analyses predicting (*A*) HLH-IRIS and (*B*) prolonged (>8 weeks) corticosteroid course at the IRIS time point. Decision trees were constructed using 12 biomarkers (IFNγ, CXCL9, CXCL10, IL-18, IL-18BP, sCD25, CD163, IL-6, CRP, IL-10, IL-27, C1q) and 2 clinical laboratory tests (ferritin, hemoglobin) with the R "ctree" package (version 4.1.2; R Foundation for Statistical Computing). Potential splits are only included in the tree model if they met the Bonferroni-adjusted *P* value for statistical significance (*P* < .05). Ovals indicate a split in the prediction rule on a specific variable, along with the corresponding *P* value. Each rectangle shows the percentage of observations within that branch that met the outcome variable. The binary outcomes of HLH versus no HLH and steroids >8 weeks (Long) versus steroids <8 weeks or no steroids (Short-None) were evaluated. Biomarker values are represented as pg/mL. Abbreviations: BP, binding protein; CRP, C-reactive protein; CXCL, C-X-C motif chemokine ligand; Hgb, hemoglobin; HLH, hemophagocytic lymphohistiocytosis; IFNγ, interferon-γ; IL, interleukin; IRIS, immune reconstitution inflammatory syndrome; sCD25, soluble CD25.

pathogenesis and an overlap in the pathophysiology between HLH-IRIS and other causes of HLH [19, 22, 29].

Cellular activation profiles highlighted a greater percentage of activated T cells in HLH-IRIS, with a concomitant decrease in Tregs. A similar dysregulated T-cell phenotype has been described as a possible mechanism of disease in HLH [20, 28, 30]. Mycobacterial IRIS is characterized by a polyfunctional expansion of CD4 T cells post-ART, but differences in Treg reconstitution have not previously been identified [9, 14]. Using our unique classification system we implicate, for the first time, an impairment in Treg reconstitution in severe IRIS pathogenesis. Genetic testing was performed in all patients and demonstrated an increased prevalence of rare, protein-altering variants in cytotoxicity genes (related to pHLH) specifically in patients with mycobacterial IRIS (unpublished observations, J.M. Rocco and I. Sereti, 2022). Similar heterozygous variants have been found at higher rates in other sHLH cohorts [31, 32], further supporting the role of HLH pathophysiology in mycobacterial IRIS.

Predicting IRIS severity is challenging as risk factors, such as pathogen burden, are difficult to quantify. Prolonged TB-IRIS with symptoms for more than 90 days has been found in up to 40% of IRIS cases [33]. CXCL9 is a surrogate marker for IFNγ activity since its production is driven by type II interferons and it can be reliably measured in peripheral blood. It is elevated in all forms of HLH and serves as a marker of disease activity [34, 35]. In our cohort, those with HLH-IRIS required prolonged corticosteroid therapy much greater than the 4 weeks utilized in randomized trials for the treatment and prevention of TB-IRIS [36, 37]. Biomarkers such as CXCL9 and sCD25 may help identify severe cases of mycobacterial IRIS and could be

incorporated into testing algorithms. Interestingly, innate immune activation markers such as CRP could not differentiate HLH-IRIS from IRIS, rendering them less helpful for prognosticating IRIS severity despite easy clinical access.

Identifying predictive markers of IRIS severity pre-ART could provide even greater clinical value as patients often present with opportunistic infections and broad corticosteroid use is associated with risks, including exacerbation of underlying KS or hepatitis B [11]. Baseline hemoglobin was the major predictor of severe inflammatory disease consistent with prior studies [1], conferring a simple clinical marker for risk stratification pre-ART. Increased ferritin, a key marker of macrophage activation, was the most differentiating clinical laboratory marker at IRIS onset in those with HLH-IRIS. Combining measurements of these common, accessible clinical tests could represent a feasible way to predict IRIS severity even in resource-limited settings.

Our study has some limitations. HLH/MAS criteria were applied retrospectively, and associated laboratory measurements were not monitored in all patients. However, this strengthens our clinical outcomes analysis since HLH-related markers were not used to make treatment decisions. We utilized all published HLH/MAS criteria, and all participants underwent detailed clinical evaluation and were followed longitudinally, decreasing the odds of misclassification. The sample size was relatively small, with an overrepresentation of minorities, likely reflecting the demographics of late HIV diagnosis. Finally, the NIH is a referral institution, raising the possibility of sampling bias.

In summary, we describe a novel relationship between severe mycobacterial IRIS and HLH/MAS demonstrating an overlapping clinical phenotype and pathophysiology driven by IFNγ
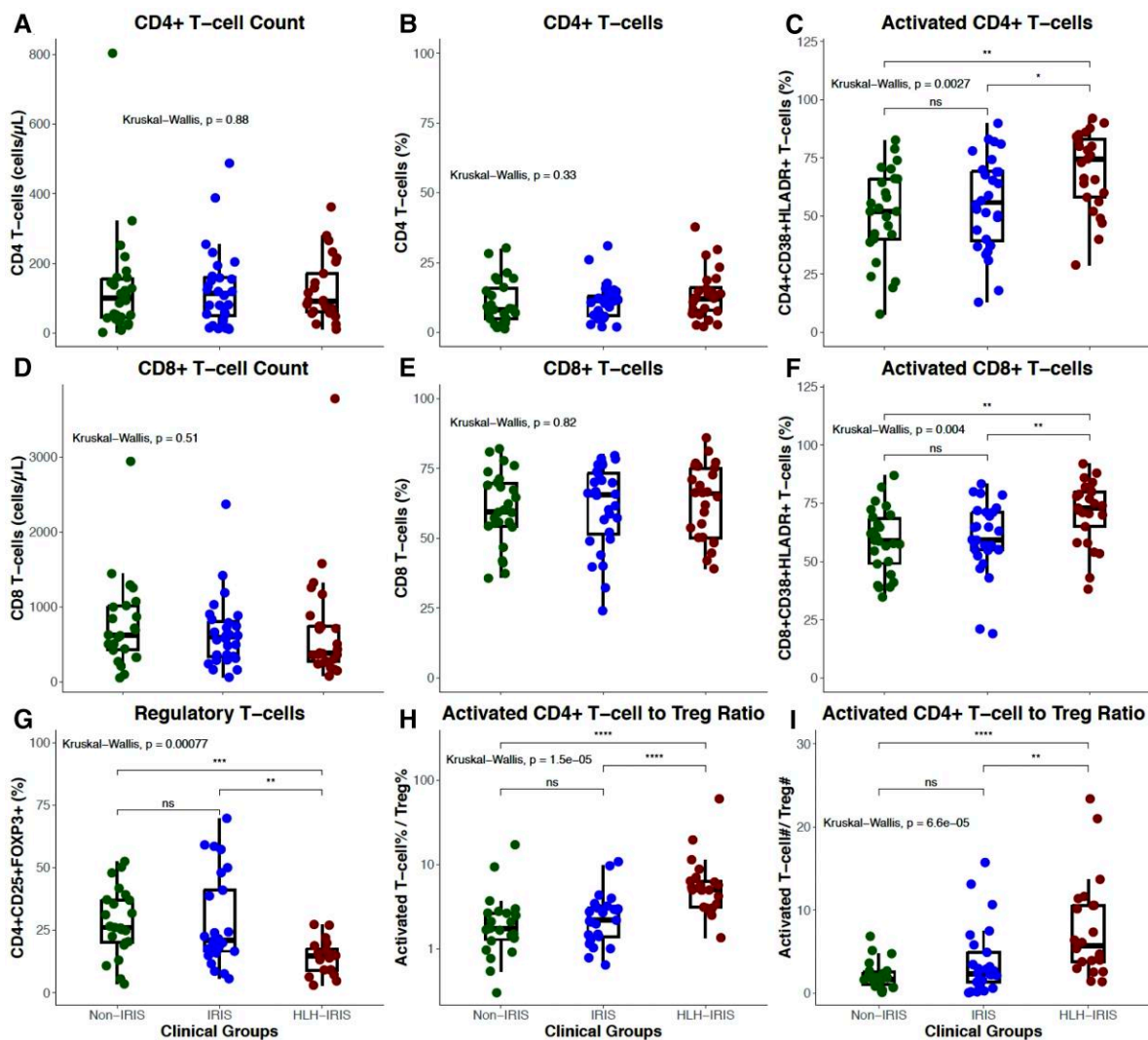
Figure 4. T-cell counts and phenotypes across the 3 study groups at the IRIS-equivalent timepoint. Data are presented as boxplots with medians and interquartile ranges. Groups were compared using the Kruskal–Wallis test and significant differences (*P* < .05) were further evaluated with pairwise Wilcoxon and Holm correction. No significant differences were noted in the percentage or absolute CD4 and CD8 T-cell counts (*A, B, D, E*). A statistically significant increase in activated CD4 (CD4$^+$CD38$^+$HLA-DR$^+$) and CD8 (CD8$^+$CD38$^+$HLA-DR$^+$) T cells was identified in the HLH-IRIS group (*C, F*). Regulatory (CD4$^+$CD25$^+$FOXP3$^+$) T cells (Tregs) were decreased in HLH-IRIS compared with the other groups (*G*), and there was an increase in the activated CD4 T-cell to Treg ratio in the HLH-IRIS cohort using cell percentages and absolute numbers (*H, I*). Abbreviations: HLH, hemophagocytic lymphohistiocytosis; IRIS, immune reconstitution inflammatory syndrome; ns, not significant. **P* < .05; ***P* < .01; ****P* < .001; *****P* < .0001.

and unopposed T-cell activation. These findings support a final common pathway involved in hyperferritinemic inflammatory syndromes from a variety of sHLH triggers, including coronavirus disease 2019 (COVID-19) and even cytokine release syndrome associated with chimeric antigen receptor (CAR) T cells [38]. Inflammasome activation with increased IL-18 is a consistent predisposing factor linking innate immune activation to adaptive T-cell dysregulation [16]. A comprehensive evaluation of diverse hyperinflammatory syndromes in adults is required to further characterize this population and identify key pathophysiologic and prognostic factors.

For this unique hyperinflammatory subset of patients with mycobacterial IRIS, a notably elevated ferritin can clinically

differentiate this group. We propose classifying this population as hyperferritinemic IRIS or FIRIS to facilitate more detailed characterization in future studies. HLH-IRIS occurred in both paradoxical and unmasking mycobacterial IRIS from TB and NTM with similar immune profiles, supporting a common converging pathophysiology consistent with other causes of sHLH [38]. This association unravels new pathways to improve the diagnosis, prognosis, and management of mycobacterial IRIS. Whole-blood assays evaluating mycobacteria-specific T-cell responses could provide greater specificity and should also be explored. The utility of biomarkers such as hemoglobin, ferritin, CXCL9, and sCD25 for IRIS prognostication should be validated in other cohorts. Confirming the utility of these
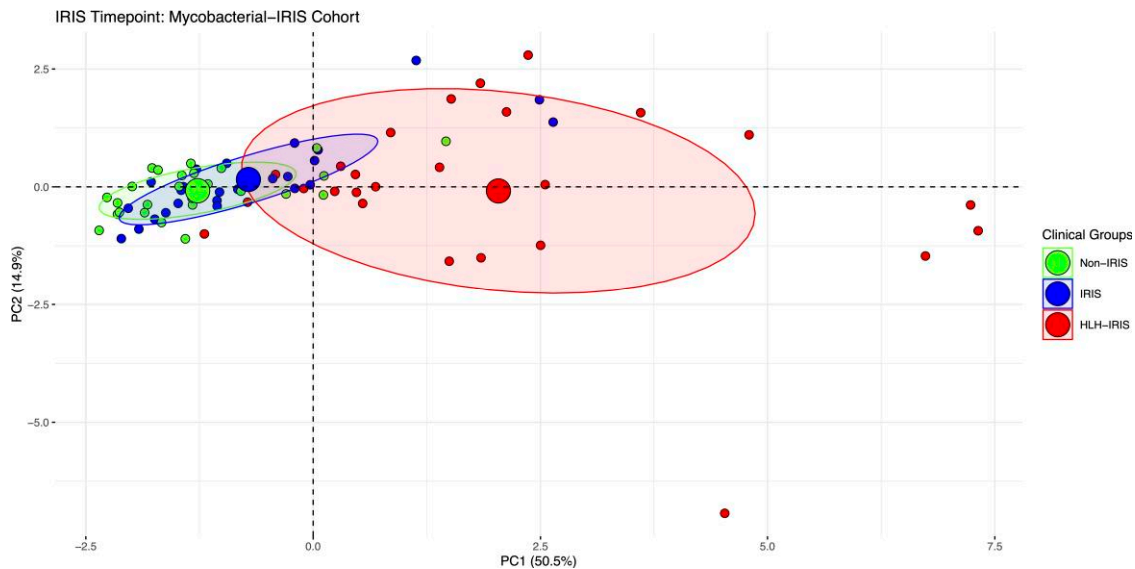
Figure 5. Multidimensional analysis of biomarkers and T-cell phenotypes distinguishes patients with HLH-IRIS from those with IRIS not meeting HLH criteria. Principal component analysis combining the IFNγ–IL-18 axis biomarkers and T-cell phenotypes (activated CD4^{+}, CD8^{+} T cells, and regulatory T cells) depicting the clustering of patients across the study groups at the IRIS time point. Individuals are represented by small colored circles for each group, whereas the overall group is represented by large colored circles. The week 4 time point was used for the non-IRIS cohort. There is a distinct separation of the HLH-IRIS cluster, emphasizing the unique pathophysiology in this subset of patients, which portends more severe inflammatory disease and the need for greater immunosuppression and close clinical monitoring. Analysis was performed in R using the FactoMineR and factoextra packages (R Foundation for Statistical Computing). Abbreviations: HLH, hemophagocytic lymphohistiocytosis; IFNγ, interferon-γ; IL, interleukin; IRIS, immune reconstitution inflammatory syndrome; PC, principal component.

markers will improve the prompt initiation of corticosteroids for high-risk patients with HLH-IRIS. Novel treatments for HLH such as oral Janus kinase (JAK) inhibitors could also be explored as steroid-sparing agents in those with mycobacterial IRIS requiring prolonged immune suppression.

Supplementary Data

Supplementary materials are available at *Clinical Infectious Diseases* online. Consisting of data provided by the authors to benefit the reader, the posted materials are not copyedited and are the sole responsibility of the authors, so questions or comments should be addressed to the corresponding author.

Notes

References

1. Sereti I, Sheikh V, Shaffer D, et al. Prospective international study of incidence and predictors of immune reconstitution inflammatory syndrome and death in people living with human immunodeficiency virus and severe lymphopenia. Clin Infect Dis **2020**; 71:652–60.
2. Benda R, David M, Franchel F, Kahn M. Multiple brain cold abscesses during pulmonary tuberculosis treated by antibiotics; proof of their tuberculous origin furnished by the surgical specimens. Bull Mem Soc Med Hop Paris **1954**; 70:802–6.
3. World Health Organization. Consolidated guidelines on HIV prevention, testing, treatment, service delivery and monitoring: recommendations for a public health approach, 2021 update. Geneva, Switzerland: World Health Organization, **2021**.
4. Quinn CM, Poplin V, Kasibante J, et al. Tuberculosis IRIS: pathogenesis, presentation, and management across the spectrum of disease. Life (Basel) **2020**; 10:262.
5. Tan HY, Yong YK, Shankar EM, et al. Aberrant inflammasome activation characterizes tuberculosis-associated immune reconstitution inflammatory syndrome. J Immunol **2016**; 196:4052–63.
6. Tan HY, Yong YK, Andrade BB, et al. Plasma interleukin-18 levels are a biomarker of innate immune responses that predict and characterize tuberculosis-associated immune reconstitution inflammatory syndrome. AIDS **2015**; 29:421–31.
7. Lai RPJ, Meintjes G, Wilkinson KA, et al. HIV-tuberculosis-associated immune reconstitution inflammatory syndrome is characterized by Toll-like receptor and inflammasome signalling. Nat Commun **2015**; 6:8451.
8. Lage SL, Wong CS, Amaral EP, et al. Classical complement and inflammasome activation converge in CD14highCD16-monocytes in HIV associated TB-immune reconstitution inflammatory syndrome. PLoS Pathog **2021**; 17: e1009435.
9. Hsu DC, Breglio KF, Pei L, et al. Emergence of polyfunctional cytotoxic CD4+ T cells in mycobacterium avium immune reconstitution inflammatory syndrome in human immunodeficiency virus-infected patients. Clin Infect Dis **2018**; 67: 437–46.
10. Andrade BB, Singh A, Narendran G, et al. Mycobacterial antigen driven activation of CD14++CD16- monocytes is a predictor of tuberculosis-associated immune reconstitution inflammatory syndrome. PLoS Pathog **2014**; 10:e1004433.
11. Walker NF, Scriven J, Meintjes G, Wilkinson RJ. Immune reconstitution inflammatory syndrome in HIV-infected patients. HIV AIDS (Auckl) **2015**; 7:49–64.

12. Vinhaes CL, Sheikh V, de-Souza DO, et al. An inflammatory composite score predicts mycobacterial IRIS in people with HIV and severe lymphopenia: a prospective international cohort study. J Infect Dis 2021; 223:1275–83.

13. Ravimohan S, Tamuhla N, Steenhoff AP, et al. Immunological profiling of tuberculosis-associated immune reconstitution inflammatory syndrome and non-immune reconstitution inflammatory syndrome death in HIV-infected adults with pulmonary tuberculosis starting antiretroviral therapy: a prospective observational cohort study. Lancet Infect Dis 2015; 15:429–38.

14. Haridas V, Pean P, Jasenosky LD, et al. TB-IRIS, T-cell activation, and remodeling of the T-cell compartment in highly immunosuppressed HIV-infected patients with TB. AIDS 2015; 29:263–73.

15. Jordan MB, Allen CE, Greenberg J, et al. Challenges in the diagnosis of hemophagocytic lymphohistiocytosis: recommendations from the North American Consortium for Histiocytosis (NACHO). Pediatr Blood Cancer 2019; 66:e27929.

16. Crayne CB, Albeituni S, Nichols KE, Cron RQ. The immunology of macrophage activation syndrome. Front Immunol 2019; 10:119.

17. Nikiforow S, Berliner N. The unique aspects of presentation and diagnosis of hemophagocytic lymphohistiocytosis in adults. Hematology Am Soc Hematol Educ Program 2015; 2015:183–9.

18. Xu XJ, Tang YM, Song H, et al. Diagnostic accuracy of a specific cytokine pattern in hemophagocytic lymphohistiocytosis in children. J Pediatr 2012; 160:984–90.e1.

19. Lin H, Scull BP, Goldberg BR, et al. IFN-gamma signature in the plasma proteome distinguishes pediatric hemophagocytic lymphohistiocytosis from sepsis and SIRS. Blood Adv 2021; 5:3457–67.

20. Chaturvedi V, Marsh RA, Zoref Lorenz A, et al. T-cell activation profiles distinguish hemophagocytic lymphohistiocytosis and early sepsis. Blood 2021; 137:2337–46.

21. Zoref-Lorenz A, Murakami J, Hofstetter L, et al. An improved index for diagnosis and mortality prediction in malignancy-associated hemophagocytic lymphohistiocytosis. Blood 2022; 139:1098–110.

22. Bracaglia C, de Graaf K, Pires Marafon D, et al. Elevated circulating levels of interferon-gamma and interferon-gamma-induced chemokines characterise patients with macrophage activation syndrome complicating systemic juvenile idiopathic arthritis. Ann Rheum Dis 2017; 76:166–72.

23. Ravelli A, Minoia F, Davi S, et al. 2016 Classification criteria for macrophage activation syndrome complicating systemic juvenile idiopathic arthritis: a European League Against Rheumatism/American College of Rheumatology/Paediatric Rheumatology International Trials Organisation Collaborative Initiative. Arthritis Rheumatol 2016; 68:566–76.

24. Fardet L, Galicier L, Lambotte O, et al. Development and validation of the HScore, a score for the diagnosis of reactive hemophagocytic syndrome. Arthritis Rheumatol 2014; 66:2613–20.

25. Henter JI, Horne A, Arico M, et al. HLH-2004: diagnostic and therapeutic guidelines for hemophagocytic lymphohistiocytosis. Pediatr Blood Cancer 2007; 48:124–31.

26. Bauchmuller K, Manson JJ, Tattersall R, et al. Haemophagocytic lymphohistiocytosis in adult critical care. J Intensive Care Soc 2020; 21:256–68.

27. Cetica V, Sieni E, Pende D, et al. Genetic predisposition to hemophagocytic lymphohistiocytosis: report on 500 patients from the Italian registry. J Allergy Clin Immunol 2016; 137:188–96, e4.

28. Humblet-Baron S, Franckaert D, Dooley J, et al. IFN-gamma and CD25 drive distinct pathologic features during hemophagocytic lymphohistiocytosis. J Allergy Clin Immunol 2019; 143:2215–26, e7.

29. Rodriguez-Smith JJ, Verweyen EL, Clay GM, et al. Inflammatory biomarkers in COVID-19-associated multisystem inflammatory syndrome in children, Kawasaki disease, and macrophage activation syndrome: a cohort study. Lancet Rheumatol 2021; 3:e574–e84.

30. Ammann S, Lehmberg K, Zur Stadt U, et al. Primary and secondary hemophagocytic lymphohistiocytosis have different patterns of T-cell activation, differentiation and repertoire. Eur J Immunol 2017; 47:364–73.

31. Kaufman KM, Linghu B, Szustakowski JD, et al. Whole-exome sequencing reveals overlap between macrophage activation syndrome in systemic juvenile idiopathic arthritis and familial hemophagocytic lymphohistiocytosis. Arthritis Rheumatol 2014; 66:3486–95.

32. Schulert GS, Zhang M, Fall N, et al. Whole-exome sequencing reveals mutations in genes linked to hemophagocytic lymphohistiocytosis and macrophage activation syndrome in fatal cases of H1N1 influenza. J Infect Dis 2016; 213:1180–8.

33. Bana TM, Lesosky M, Pepper DJ, et al. Prolonged tuberculosis-associated immune reconstitution inflammatory syndrome: characteristics and risk factors. BMC Infect Dis 2016; 16:518.

34. De Benedetti F, Prencipe G, Bracaglia C, Marasco E, Grom AA. Targeting interferon-gamma in hyperinflammation: opportunities and challenges. Nat Rev Rheumatol 2021; 17:678–91.

35. Verweyen EL, Schulert GS. Interfering with interferons: targeting the JAK-STAT pathway in complications of systemic juvenile idiopathic arthritis (SJIA). Rheumatology (Oxford) 2022; 61:926–35.

36. Meintjes G, Wilkinson RJ, Morroni C, et al. Randomized placebo-controlled trial of prednisone for paradoxical tuberculosis-associated immune reconstitution inflammatory syndrome. AIDS 2010; 24:2381–90.

37. Meintjes G, Stek C, Blumenthal L, et al. Prednisone for the prevention of paradoxical tuberculosis-associated IRIS. N Engl J Med 2018; 379:1915–25.

38. Schulert GS, Canna SW. Convergent pathways of the hyperferritinemic syndromes. Int Immunol 2018; 30:195–203.